

Scientific paper

Effect of Chloride and Sulfate in the Immobilization of Cs-137 in C-S-H Gel

Eduardo Duque-Redondo^{1*}, Kazuo Yamada² and Hegoí Manzano³

Received 14 September 2020, accepted 22 December 2020

doi:10.3151/jact.19.95

Abstract

Cementitious materials are commonly used in nuclear repository sites to immobilize intermediate-level radioactive wastes. This is due to the large surface area of the calcium silicate hydrate (C-S-H) gel, the main hydration product of ordinary Portland cement, which provides many sorption sites in which the contaminants can be adsorbed. The retention capacity of these materials is strongly dependent on the composition, the water content, the pH or the presence of additives. Likewise, it is also known that the durability and performance of cement and concrete are adversely affected in chloride and/or sulfate environments. In this work, atomistic simulations have been employed to analyze the effect of the presence of chlorides and sulfates in the retention and transport of ¹³⁷Cs, one of the most hazardous radioisotopes, in calcium silicate hydrate. The simulations suggest that the presence of a moderate amount of chlorides does not alter significantly the Cs uptake in C-S-H gel, while a moderate content of sulfates enhances substantially the retention of Cs ions and reduces their migration throughout the pore. This behavior is attributed to the ability of the sulfates to pull Ca out the high-affinity sites from the C-S-H surface, allowing Cs ions to occupy them.

1. Introduction

The development of nuclear reactors for energy production revealed the great advantages offered by this energy source, among which it can be highlighted the high reliability and the low cost of energy production. However, nuclear energy generation involves many challenges that need to be addressed. The most prominent is the safe management, storage and disposal of the radioactive wastes produced in the nuclear facilities. The most common nuclear fuel contains isotopes of uranium and plutonium that produce different fission products. Many of these products are either non-radioactive or short-lived radioisotopes, but some of them are dangerous and/or long-lived radioisotopes. The end products ⁹⁰Sr and ¹³⁷Cs are the most hazardous radioisotopes from the spent nuclear fuel and constitute the main source of radiation released after the Chernobyl and Fukushima incidents (Real *et al.* 2004; Amano *et al.* 2012). However, the ease of spreading of ¹³⁷Cs due to its high volatility and solubility (Jantunen *et al.* 1991) facilitates the uptake of this radioisotope in the food chain with the subsequent risks for humans and animals,

so the isolation of this radioisotope deserves especial attention.

The processing of the spent nuclear fuel involves several steps, including the segregation of the radioactive components from the bulk waste and the conditioning process to convert the raw radioactive waste into stable solid forms or waste forms. In this way, the conditioning process aims to immobilize the mobile contaminants by solidification, embedding or encapsulation methods in order to minimize their potential dispersion and migration (Palmer and Fairhall 1992; Krishnamoorthy *et al.* 1993). Cementation (Coumes and Courtois 2003), bituminization (Kluger *et al.* 1980) and vitrification (Lee *et al.* 2006) are common techniques for the immobilization of low- and intermediate-level radioactive wastes, the former being the most used worldwide (Barinov *et al.* 1990; Coumes and Courtois 2003; Rahman *et al.* 2014), in which the immobilization occurs by precipitation and adsorption of the mobile contaminants (Macáček 1999; Real *et al.* 2002).

Ordinary Portland cement, OPC, is commonly used for cementation (Glasser and Atkins 1994) since the calcium silicate hydrate or C-S-H gel, the main hydration product of OPC, has a large surface area with many sorption and reaction sites in which the contaminants can be retained (Real *et al.* 2002; Volchek *et al.* 2011). Moreover, the C-S-H gel has low diffusibility and solubility due to its microstructure, which reduces the mobility of the contaminants and prevents their release (Hewlett 2003; Kiran *et al.* 2020).

The studies on Cs uptake in cementitious materials revealed that the retention distribution, R_d , varies several orders of magnitude depending on the experimental conditions. These studies indicate that the Cs uptake on C-S-H gel can be increased by lowering the Ca/Si ratio

¹Researcher, Department of Physical Chemistry, University of the Basque Country UPV/EHU, Aptdo. 664, 48080, Bilbao, Spain. *Corresponding author, E-mail: eduardo.duque@ehu.eus

²Senior Researcher, Fukushima Branch, National Institute for Environmental Studies, Miharu, Tamura, Fukushima, 963-7700, Japan.

³Assistant Professor, Department of Physics, University of the Basque Country UPV/EHU, Aptdo. 664, Bilbao, Spain.

and rising the Al/Si ratio (Bagosi and Csetényi 1998; Ochs *et al.* 2015; Duque-Redondo *et al.* 2018a, 2021). Likewise, acid pH enhances the retention of Cs since at basic pH there is a higher content of calcium hydroxide that can saturate the sorption sites from the C-S-H surface (Glasser 1993; Ochs *et al.* 2015). The use of additives, such as silica fume or clays, in combination with the OPC, also influences the Cs uptake and its leaching since they may induce changes in the porous structure and water content, which may result in a difference in the Cs diffusivity of several orders of magnitude (Atkinson and Nickerson 1984; Johnston and Wilmot 1992; El-Kamash *et al.* 2002).

The cementation technique has proved to isolate the radioactive contaminants safely for a long time. However, these species would be eventually released by the action of different factors. For instance, chloride and sulfate attacks are aggressive deterioration mechanisms that affect the long-term durability of cement and concrete structures and can cause the fracture of the waste-forms, facilitating the intrusion of groundwater and the release of the contaminants (Atkinson and Hearne 1989). Many studies have been analyzed on the effects that the presence of chlorides and sulfates have on the durability and mechanical performance of cement-based materials (Neville 1995; Al-Amoudi 2002; Stroh *et al.* 2016; Ramezani-pour and Riahi Dehkordi 2017), but they do not focus on the impact of these species on Cs uptake in calcium silicate hydrates.

In this work, the authors have analyzed by means of molecular dynamics simulations the impact of the presence of chlorides and sulfates in the C-S-H nanopores on the Cs uptake and its diffusivity. To this effect, the authors have developed three C-S-H models with Ca/Si ratio of 1.67, the average ratio in Portland cement paste, and pore size of 1 nm, in which Cs is introduced with a concentration of 1.68 Cs per nm² of C-S-H surface counterbalanced by hydroxyl groups, chlorides and sulfates, respectively. The atomistic simulations have been analyzed to characterize the distribution of the confined species in the nanopore in the presence of the considered counterions, along with the type and number of sorption sites available on the C-S-H surfaces for Cs and Ca ions. The transport properties of Cs, Ca and water molecules are also evaluated by computing their diffusion coefficients.

2. Simulation details

The C-S-H models have been built following the procedure described by Kovačević *et al.* (2016) for Model 1, although the 14 Å-tobermorite's structure (Bonaccorsi *et al.* 2005) was used as a starting point instead of 11 Å-tobermorite's structure. These two polytypes differ mainly on the basal spacing and the water content, higher in 14 Å-tobermorite. Moreover, in 11 Å-tobermorite the silicate chains from adjacent layers can be linked by condensation of bridging sites (Q³ silicate species). The

structure of 14 Å-tobermorite has been employed as a starting point to develop our models because the water content is more similar to that of C-S-H gel and there are no Q³ silicate species (Rejmak *et al.* 2012; Cuesta *et al.* 2018). Kovačević's procedure involves the omission of bridging silicates in the tobermorite's infinite silicate chains and the addition of Ca ions into the interlaminar space to reach the target Ca/Si ratio (1.67), as in previous works (Duque-Redondo *et al.* 2018a, 2018b). Thus, the initial 14 Å-tobermorite's unit cell was replicated to obtain a simulation box with dimensions of 2.6 × 3.1 × 3.3 nm³, corresponding to the x-, y- and z-axes, and periodic boundary conditions were applied. Then, water was removed from the interlaminar spaces and the Ca/Si ratio was increased from 0.83, the value in 14 Å-tobermorite, to 1.67, deleting randomly some bridging silicates and adding Ca in the interlaminar space. The silicate omission creates defects on the C-S-H in which the added Ca ions can be accommodated (Kumar *et al.* 2017). Then, water was reintroduced and the C-S-H model was relaxed by performing an energy minimization and equilibration in the isobaric-isothermal ensemble (NPT) for 5 ns at 300 K using a reactive force field, ReaxFF (Chenoweth *et al.* 2008; Fogarty *et al.* 2010; Manzano *et al.* 2012b), which allows the dissociation of water molecules in dangling oxygen atoms from the new Q¹ sites, created by the omission of the bridging silicates.

Once the C-S-H model was equilibrated, the interlaminar space was opened 1 nm to create a gel pore in which one can study the retention and transport of Cs (Pinson *et al.* 2015). The authors have selected this width as a limit case since Pinson *et al.* suggested that above 1 nm, there is a change in water properties; in smaller pores or interlayer spaces (below 1 nm) the electrostatic confinement is so high that the mobility of the water molecules is very constrained, while above 1 nm water can flow and, in turn, all the species confined on the pore, like the Cs ions. Thus, in pores above 1 nm, there might be leaching processes that result in the release of the confined contaminants. In the expanded pore space, Cs ions counterbalanced with hydroxyls, chlorides and sulfates, were introduced with a concentration of 1.68 Cs per nm² of C-S-H surface, equivalent to a Cs/Ca ratio of 0.85, the value found experimentally in 14 Å-tobermorite (Miyake *et al.* 1989). It must be noted that, regardless of the counterion, all the systems contain hydroxyl groups coming from the water dissociation. Finally, the pore is filled with water up to 1 g·cm⁻³ using a geometry-based algorithm (Martínez and Martínez 2003; Martínez *et al.* 2009) and the three systems (the first one counterbalanced with hydroxyl, the second one with chlorides and the third one with sulfates) were equilibrated again by running a new energy minimization and molecular dynamics simulations. The equilibration has been performed using a combination of CSHFF force field (Shahsavari *et al.* 2011) to describe the C-S-H structure, ClayFF (Cygan *et al.* 2004)

Table 1 Comparison of the final properties of the structure of the C-S-H before expanding the interlaminar space, obtained from our simulations and the literature.

	This work	Literature
Ca/Si	1.67	1.67
MCL (Cong and Kirkpatrick 1996; Chen <i>et al.</i> 2004; Dolado <i>et al.</i> 2007; Qomi <i>et al.</i> 2014)	2.4	2.1 to 3.0
H ₂ O/Si (Fujii and Kondo 1981; Cong and Kirkpatrick 1996; Thomas <i>et al.</i> 2003; Qomi <i>et al.</i> 2014)	2.5	2.3 to 3.2
Ca-OH/Ca (Fujii and Kondo 1981; Thomas <i>et al.</i> 2003; Dolado <i>et al.</i> 2007; Qomi <i>et al.</i> 2014)	0.37	0.27 to 0.44
Si-OH/Si (Cong and Kirkpatrick 1996; Dolado <i>et al.</i> 2007)	0.15	0.10 to 0.21

for the Cs and Cl ions and CHARMM force field (Brooks *et al.* 1983; Vanommeslaeghe *et al.* 2010) for the sulfates. After the energy minimization, the systems were initially relaxed in the canonical ensemble (NVT) at 300 K with a thermostat coupling constant of 0.1 ps during 0.5 ns and using a time step of 0.5 fs. Then, further relaxation was performed by running another 0.5 ns simulation in the isobaric-isothermal ensemble (NPT) at 300 K and 1 atm with a barostat coupling of 1 ps. Finally, a 50 ns simulation is run in the canonical ensemble (NVT) at 300 K. LAMMPS code (Plimpton 1995) was used to run the MD simulations, while the integration of the motion equation and the long-range Coulombic interaction were computed using the Verlet algorithm (Verlet 1967) and the Ewald summation method (Ewald 1921).

3. Results and discussion

3.1 C-S-H model structure

As mentioned before, the C-S-H models employed in this work, have been built following the procedure described by Kovačević *et al.* (2015, 2016), which derives from the procedure of Qomi *et al.* (2014). These authors performed a thorough and rigorous validation of the C-S-H models, comparing the structural parameters and elastic properties with experimental samples. Thus, one can assume those validations for our models. Nevertheless, for further validation, the structural parameters of the equilibrated C-S-H model with a Ca/Si ratio of 1.67 obtained from the molecular dynamics simulation before expanding the interlaminar space have been compared with the values reported by other authors for experimental and simulated C-S-H samples with the same Ca/Si ratio. This comparison is shown in **Table 1** and it can be seen that our model is in line with the systems reported by other authors. It must be noted that the composition of the C-S-H gel (Ca/Si and H₂O/Si ratios) and the mean chain length (MCL) have been defined to replicate the experimental values of C-S-H systems reported in the literature, while the Si-OH/Si (Si-OH bonds per Si atom) and Ca-OH/Ca (Ca-OH bonds per Ca atom) ratios result from the chemical relaxation provided by the reactive force field ReaxFF.

3.2 Nanopore arrangement

The distribution of the confined species in the C-S-H nanopore can be explored by computing the atomic density profiles of the modeled systems. This tool gives the density of a given particle or molecule as a function of the distance from a plane. Thus, it can be used to monitor the distribution of the water molecules, cations and counterions throughout the pore, in the z-direction, perpendicular to the C-S-H surfaces. **Figure 1** shows the atomic density profiles of water, Ca, Cs and the corresponding counterions (hydroxyl groups, chlorides and sulfates) along with a snapshot of the system for better comprehension. These atomic density profiles were obtained averaging and normalizing the atomic positions for 20 ns.

In **Fig. 1**, only the interphase, in which water penetrates into the solid C-S-H (between approximately -2.5 Å and 0 Å) and the bulk liquid region (above 0 Å) are shown, while the bulk solid (C-S-H) region is omitted. This classification has been done according to the Guggenheim convention (Guggenheim 1985), which divides the systems into those three regions and defines two interfacial limits: the lower and the upper interfacial limits (LIL and UIL), which are the imaginary boundaries between the interphase and the bulk solid and bulk liquid phases, respectively. In **Fig. 1**, the authors have assigned to the upper interfacial limit (UIL) the value 0 Å, while the lower interfacial limit (LIL) is not represented, but it is placed at about -2.5 Å.

The atomic density profiles exhibit significant differences in the distribution of the cations and counterions. On the one hand, it can be seen that hydroxyl groups can be found both above and below the upper interfacial limit, while sulfates are mainly located above the upper interfacial limit and chloride ions are exclusively located in the bulk liquid region. On the other hand, the distribution of the cations is altered by the counterion present in the pore: while the distribution of Cs and Ca ions counterbalanced by hydroxyl groups and chloride ions is similar, finding these cations both below and above the upper interfacial limit, when sulfates are present, the amount of Ca ions in the interphase is considerably lower, while the amount of Cs in the proximities of the upper interfacial limit is much higher than when it is counterbalanced by hydroxyl and chloride anions.

Table 2 Average coordination numbers for Cs and Ca to oxygen atoms from the C-S-H surface (Os), water molecules (Ow) and the counterions (hydroxyl, Oh; chloride, Cl; and sulfates, SO₄) for the three considered systems.

Main counterion	Cs			Ca		
	Oh	Cl	SO ₄	Oh	Cl	SO ₄
Os	1.9	1.8	2.5	3.0	2.9	2.3
Ow	5.3	5.1	4.7	1.8	2.1	2.2
Oh	1.1	0.6	0.6	2.3	2.0	1.7
Cl	-	0.7	-	-	0.1	-
SO ₄	-	-	0.4	-	-	0.8
Total	8.3	8.2	8.2	7.1	7.1	7.0

3.3 Local structure

The atomic density profiles have revealed significant differences in the distribution of Cs and Ca in the C-S-H nanopore. These differences should be reflected in the local structure of the cations. Thus, radial distribution functions (RDFs) and coordination numbers (CNs) of Cs and Ca in each system to characterize their average local structure have been computed, as can be seen in **Fig. 2**.

It can be seen that the radial distribution functions and coordination numbers of Cs and Ca ions are very different. This is due to the differences in the size and charge of those cations. Cs ions have low charge density since they are large and monovalent cations, while the charge density of Ca is much higher due to its smaller size and higher charge. The diffuse charge of Cs results in wide peaks in the RDFs and ill-defined coordination numbers, whereas Ca, with high charge density, exhibits sharp peaks and well-defined coordination numbers. The size of the cations is also reflected in the M-X distances,

finding larger Cs-X distances in comparison with Ca-X distances. For instance, the average Cs-O distance is about 3.1 Å, while the average Ca-O distance is 2.5 Å. These values are in agreement with the experimental M-O distances, ranging from 3.0 to 3.3 Å (Schwenk *et al.* 2004; Mähler and Persson 2011) for Cs-O and from 2.4 to 2.5 Å (Abriel 1983; Bako *et al.* 2002; Kubillus *et al.* 2014) for Ca-O. Likewise, the Cs-Cl distance, 3.6 Å, is larger than the Ca-Cl distance, 2.8 Å, both values in the line of the distance measured experimentally, with values of 3.7 Å (Zachariassen 1948) and 2.9 Å (Chiu *et al.* 2010), respectively.

Regarding the coordination numbers, it can be seen that the coordination shell of Cs ions is significantly higher than that of Ca ions. The average coordination numbers for Cs and Ca obtained from **Fig. 2** are displayed in **Table 2** for better visualization. It must be noted that the values for Cs ions cannot be assigned unequivocally since they are ill-defined due to the diffuse

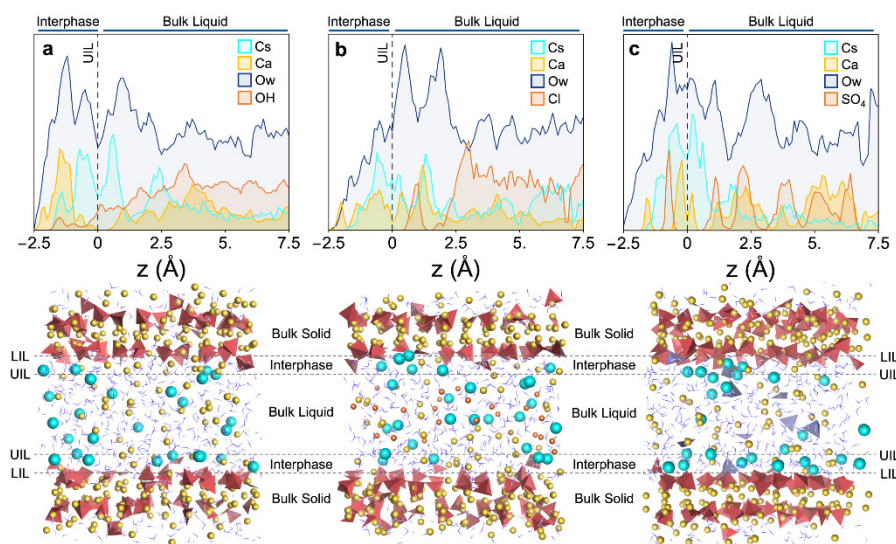


Fig. 1 Atomic density profiles and their corresponding snapshots for the systems in which Cs ions are counterbalanced with (a) hydroxyl groups, (b) chlorides and (c) sulfates. In the density profiles (upper row of figures), the black dashed line represents the upper interfacial boundary (UIL), while the profiles of Cs, Ca, water molecules and counterions are plotted in light blue, yellow, dark blue and orange, respectively. The garnet tetrahedrons of the snapshots (lower row of figures) correspond to the silicate chains, whereas the light blue and yellow balls are the Cs and Ca ions. Water and hydroxyl groups are illustrated as double and simple blue sticks. Chloride and sulfate ions are represented as orange balls and purple tetrahedrons, respectively. The lower and upper interfacial limits (LIL and UIL) are represented with black dashed lines.

charge of these cations. Nevertheless, the authors have estimated that the total coordination number for Cs ions is approximately 8.2 in the line with the values reported by other authors for Cs in bulk water, which range from 7.8 to 8.7 (Hofer *et al.* 2004; Schwenk *et al.* 2004; Mähler and Persson 2011). The total coordination number for Ca is about 7.1, a similar value to the values reported in the literature, between 7.0 and 7.4 (Bako *et al.* 2002; Hofer *et al.* 2004). Remarkably, the total coordination number of Cs and Ca remains almost constant for all the systems, although the composition of the first coordination shell changes depending on the counterion. On the one hand, the respective coordination shells of Cs and Ca in the systems counterbalanced by hydroxyls and by chlorides are similar: Cs ions are coordinated to approximately 2 atoms from the surface and 5 water molecules, completing the coordination shell with the counterions, while the coordination shell of Ca is composed of 3 oxygens from the C-S-H surface, about 2 water molecules and a little more than 2 counterions. On the other hand, the coordination shell of Cs and Ca in presence of sulfates is substantially different, finding that Cs ions increase their coordination to the C-S-H surface, while the coordination of Ca to the surface decreases significantly regarding the other two systems. It must be remembered that the atomic density profile for the system counterbalanced with sulfates shows an increase in the amount of Cs in the proximities of the C-S-H surface and a decrease of Ca in this region with regard to the other two systems. This explains the higher and lower coordination of Cs and Ca, respectively, to the C-S-H surface in presence of sulfates. Moreover, Ca is coordinated to nearly one sulfate counterion, suggesting that these counterions may pull Ca ions out from the C-S-H surface to the bulk liquid region and allowing to Cs ions occupy the high-affinity sites of the surface left by the Ca. The affinity of sulfates for Ca might be attributed to the

higher charge of Ca (divalent cation) regarding Cs (monovalent cation), which allow the formation of stronger electrostatic interactions between the sulfates and Ca ions. This is in agreement with the experimental observations of sulfate attack in cement and concrete, in which the sulfate that penetrates into these materials interact with Ca ions to form CaSO_4 or gypsum (Al-Amoudi 2002).

3.4 Sorption configuration

As has been seen, the arrangement of the cations in the C-S-H nanopore affects their average coordination shell. Thus, the contribution of the oxygen atoms from the C-S-H surface to the coordination shell of the cations located in the interphase must be substantial, while for those cations in the center of the pore, far from the surface, should be negligible. This is not trivial since affects the retention and migration of the confined species: a cation located close to the C-S-H surface that establishes strong interactions with their oxygen atoms is well retained and its mobility is restricted, while the cations in the pore that do not interact with the surface are not retained at all and they can move freely through the pore.

Many authors have classified the cations confined in the C-S-H gel into three categories according to their proximity to the surface and their coordination shell: inner-sphere complexes, outer-sphere-complexes and non-adsorbed cations (Payne *et al.* 2013; Androniuk *et al.* 2017; Jiang *et al.* 2017; Duque-Redondo *et al.* 2018b). Non-adsorbed cations are far from the C-S-H, so they do not interact with the surface's atoms and their coordination shell is mainly composed of water molecules and complete it with the counterions. Outer-sphere complexes maintain a hydration shell similar to that of non-adsorbed cations, although they are close enough to the C-S-H surface to direct coordinate to it. Finally, in inner-sphere complexes, the coordination to the C-S-H

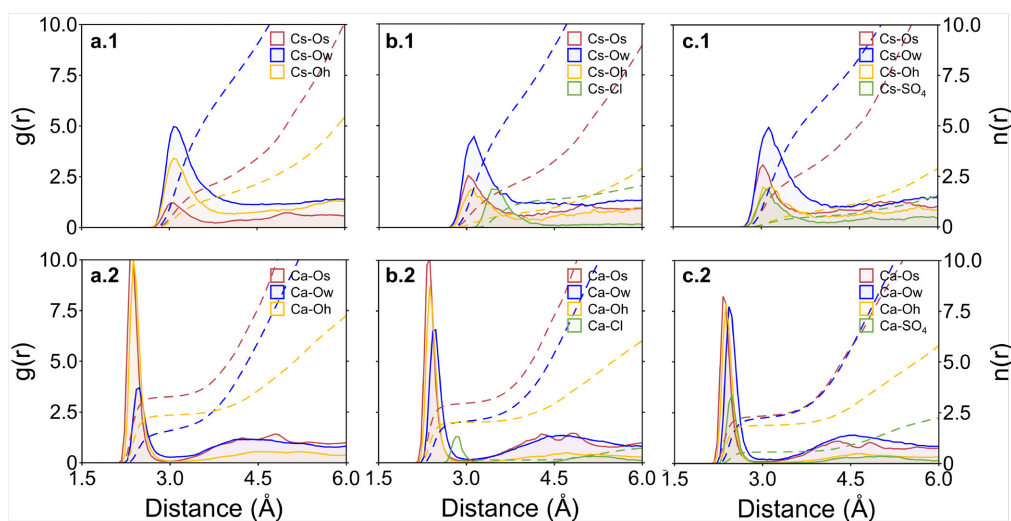


Fig. 2 Radial distribution functions (continuous lines) and coordination numbers (dashed lines) for Cs (upper row of figures) and interlayer Ca (lower row of figures) ions with (a) hydroxyl, (b) chloride, and (c) sulfate counterions. M-surface oxygen (M-Os) $g(r)$ and $n(r)$ are shown in red, M-water molecules (M-Ow) in blue, M-hydroxyl groups (M-Oh) in yellow, and M-chloride/sulfate (M-Cl/M-SO₄) in green.

Table 3. Percentage of cations adsorbed in inner-sphere and outer-sphere configurations and the non-absorbed (pore) ions in C-S-H for Cs and Ca ions counterbalanced by hydroxyls (OH), chlorides (Cl) and sulfates (SO₄).

Counterion	Cs			Ca		
	Inner	Outer	Pore	Inner	Outer	Pore
OH	32%	25%	43%	46%	12%	42%
Cl	27%	32%	41%	27%	33%	40%
SO ₄	38%	33%	29%	21%	18%	61%

Table 4. Number of inner-sphere and outer-sphere sorption sites per nm² of C-S-H and the sum of them for Cs and Ca counterbalanced by hydroxyls (OH), chlorides (Cl) and sulfates (SO₄). The total number of Cs and Ca ions is the same in all the systems, equivalent to 1.68 Cs and 3.11 Ca per nm² of C-S-H surface.

Counterion	Cs			Ca		
	Inner	Outer	Sum	Inner	Outer	Sum
OH	0.54	0.42	0.96	1.43	0.37	1.80
Cl	0.45	0.53	0.98	0.84	1.03	1.87
SO ₄	0.64	0.55	1.19	0.65	0.56	1.21

surface is much higher than in outer-sphere complexes since they are located much closer to the C-S-H surface.

Since the formation of these complexes can be related to their distance to the C-S-H surface, the Guggenheim convention can be used to facilitate the classification of the cations in these sorption configurations. Thus, non-adsorbed (pore) cations, which must be located far from the surface, are placed in the center of the bulk liquid region, while the outer-sphere complexes are associated with those cations located in the bulk liquid region but close to the surface, to the upper interfacial limit, in which they can coordinate directly to the surface and maintain high coordination to water molecules. Finally, the cations located in the interphase can be related to the inner-sphere complexes since they are embedded into the solid enabling high coordination to the C-S-H surface. However, it should be noted that at high Ca/Si ratios, as the one considered in this study (1.67), the C-S-H surface is very irregular due to the deletion of silicate groups performed during the construction of the C-S-H model drawing from the crystalline structure of 14 Å-tobermorite. Thus, these surface defects make the limits between the three regions defined by the Guggenheim convention become more diffuse, impeding to classify unequivocally the cations based solely on their location in the pore gel. Therefore, one must also analyze their local structure to classify appropriately the cations in each sorption configuration. The relative amount of Cs and Ca adsorbed in inner-sphere and outer-sphere sorption sites is given in **Table 3**, as well as the number of cations solvated in the nanopore of C-S-H, called pore cations.

Table 3 reveals that the amount of non-adsorbed Cs and Ca is similar when they are counterbalanced by hydroxyl or chlorides, although there are differences in the distribution in inner- and outer-sphere sorption configurations. However, in presence of sulfates, the amount of non-adsorbed Cs is considerably fewer than in the other two systems, while the opposite trend is found for

Ca, increasing remarkably the amount of non-adsorbed Ca in the line with the distribution found in the atomic density profiles. One can also estimate the effect of the counterion in the number of each sorption sites per unit area of C-S-H surface available for Cs and Ca, as shown in **Table 4**.

From these data, it can be seen that the total number of sorption sites for Cs and Ca is essentially the same when they are counterbalanced by hydroxyls and chlorides, while in presence of sulfates the total number of sorption sites in the C-S-H surface is almost a 25% higher for Cs ions and 34% lower for Ca. The difference in the number of sorption sites for Cs and Ca with sulfates can be attributed to the interaction of the Ca ions and the sulfates counterions in the pore. Both species are divalent and can establish stronger electrostatic interactions than with monovalent species, such as Cs, hydroxyls or chlorides. In this way, the sulfates might pull out Ca from the high-affinity sites, which can be occupied by Cs ions, resulting in higher desorption of Ca and higher adsorption of Cs in inner- and outer-sphere sorption sites. Thus, the presence of a moderate amount of sulfates may enhance Cs retention, although it might affect the performance and durability of the materials due to the formation of gypsum (CaSO₄) (Al-Amoudi 2002).

3.5 Diffusion coefficients

The migration of the cations through the C-S-H nanopore can be analyzed by computing the mean square displacement (MSD) (Brehm and Kirchner 2011). From the MSD, the diffusion coefficients (D) are obtained through the Einstein relationship (Einstein 1905):

$$D = \frac{1}{2d} \lim_{t \rightarrow \infty} \frac{MSD}{t} \quad (1)$$

where d is the dimensionality of the system.

The average diffusion coefficients of Cs, Ca and water molecules were computed and compared their values in

presence of the three considered counterions in order to investigate how the counterion type affects the migration of these species. The comparison of the diffusion coefficients of the cations and water molecules is shown in Fig. 3.

Figure 3 shows that the diffusivity of Cs ions counterbalanced with sulfates is nearly half of that of Cs ions counterbalanced with hydroxyl or chlorides. This is due to the higher amount of Cs in inner-sphere and outer-sphere sorption configurations, in which the cations can establish strong electrostatic interactions with the C-S-H surface that reduce their mobility and result in lower diffusion coefficients, especially in inner-sphere configurations, in which the interaction with the surface is much higher than in outer-sphere sorption sites. Thus, the lower diffusivity of the cations counterbalanced with hydroxyls regarding those counterbalanced by chlorides may be attributed to the higher proportion of inner-sphere complexes in the former system. In any case, the diffusivity of Cs ions confined in C-S-H nanopores is three orders of magnitude lower than in bulk water [$2.1 \times 10^{-9} \text{ m}^2 \text{ s}^{-1}$ (Yuan-Hui and Gregory 1974)] and this is due to the structural and electrostatic confinement effect caused by the inclusion in the nanopore (Kalinichev *et al.* 2007; Manzano *et al.* 2012a; Qomi *et al.* 2014; Bonnaud *et al.* 2016). On the other hand, the diffusion coefficients of interlayer Ca ions are one order of magnitude lower than the coefficients of Cs ions, which is attributed to the higher charge density of Ca ions, which allows establishing stronger interactions that reduce their potential migration.

Figure 3 also shows the diffusivity of water molecules and it can be seen that there are minor differences in their diffusion coefficients depending on the counterion that might be related to the ability of those counterions to form hydrogen bonds. In contrast to chlorides, hydroxyls and sulfates can form hydrogen bonds with water and with oxygen atoms from the surface, which can reduce the mobility in the nanopore, although the decline is not meaningful. The nanoconfinement effect is also reflected in the water diffusivity since the average diffusion coefficient for water in the C-S-H nanopore, $2.9 \times 10^{-12} \text{ m}^2 \cdot \text{s}^{-1}$, is three orders of magnitude lower than the bulk water diffusivity measured by experiments [$2.3 \times 10^{-9} \text{ m}^2 \cdot \text{s}^{-1}$ (Krynicky *et al.* 1978)] and simulations [$2.5 \times 10^{-9} \text{ m}^2 \cdot \text{s}^{-1}$ (Mahoney and Jorgensen 2001)].

4. Conclusions

In this work, the authors have investigated the impact of the presence of different counterions in the Cs uptake on C-S-H gel. In particular, the authors have studied adsorption and transport of Cs and Ca ions confined in a 1 nm gel pore of C-S-H with Ca/Si ratio of 1.67, in which Cs has been introduced at a concentration of 1.68 Cs per nm^2 of C-S-H surface counterbalanced by three different species: hydroxyl groups, chlorides and sulfates.

The analysis of the distribution of the confined species throughout the pore shows significant differences depending on the counterions, finding a higher Ca desorption and Cs adsorption in presence of sulfates than in presence of hydroxyl or chlorides. The characterization of the local structure of Cs and Ca has revealed that the first coordination shell of these cations is similar when Cs is counterbalanced with hydroxyl and chlorides, but in presence of sulfates, the coordination of Cs to the surface increases, while decreases the coordination to water molecules and counterions. The opposite behavior is found for Ca ions, in which is observed a significant decrease of the coordination number to the C-S-H surface, which is compensated by increasing the coordination to the water and the sulfate counterions, suggesting that sulfates may pull Ca out to the pore space, leaving their high-affinity sites on the C-S-H surface available for Cs ions, whose retention is enhanced in presence of this counterion.

The type and number of sorption sites on the C-S-H surface are also analyzed as a function of the counterion, finding that the total number of sorption sites per area for Cs ions is 25% higher in presence of sulfates (1.19 sites/ nm^2) than with hydroxyls and chlorides (0.96 to 0.98 sites/ nm^2). By contrast, the total number of sorption sites for Ca ions decreases up to 34% in presence of sulfates (1.21 sites/ nm^2) regarding the systems counterbalanced by hydroxyl and chlorides (1.80 to 1.87 sites/ nm^2). These data confirm that Ca is partially desorbed in presence of sulfates, allowing Cs to occupy the high-affinity sites left by the desorbed Ca. This desorption is attributed to the strong electrostatic interactions that take place between the divalent species Ca^{2+} and SO_4^{2-} , which suggests the formation of gypsum, CaSO_4 , whose formation has been observed during sulfate attack in cement and concrete. The differences in the sorption configurations regarding the counterion are reflected in

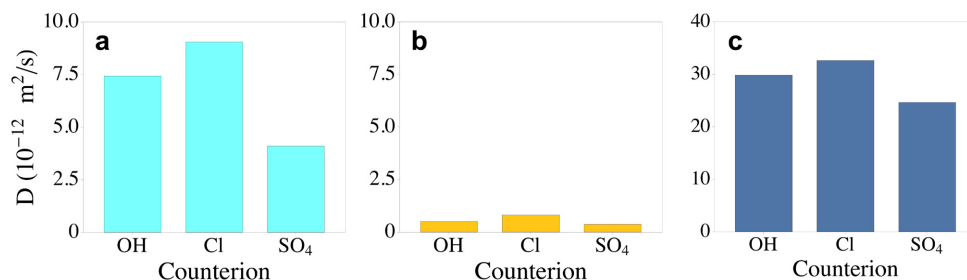


Fig. 3 Average diffusion coefficients of (a) Cs ions, (b) Ca ions and (c) water molecules as a function of the counterion. It should be noted that the scale of the diffusion coefficients is different for the cations and water.

the diffusivity of Cs ions. Thus, the higher retention of Cs counterbalanced with sulfates results in diffusion coefficients approximately 50% lower than Cs counterbalanced with hydroxyl or chlorides.

Therefore, this work has shown that the presence of moderate amounts of sulfates in the C-S-H nanopores may contribute to enhance the Cs retention and reduce its migration and potential release due to the ability of sulfates to release sorption sites from the C-S-H surface that were occupied by Ca ions. This is in agreement with the decalcification of silicate hydrates observed experimentally when sulfates penetrate through the matrix of cement and concrete, causing the formation of gypsum and ettringite that can affect the performance and durability of these materials. On the other hand, the presence of chloride counterions does not appear to have significantly affected to Cs retention and diffusion. It is also observed that the Cl counterions are not retained by the C-S-H surface, confirming that the C-S-H gel does not protect against the corrosion of the steel bars embedded in reinforced concrete.

The output from these simulations can be used to qualitatively understand the experimental results and/or guide new experiments on ionic adsorption in presence of chlorides and sulfates. Moreover, some results, such as the diffusion coefficients can be used as quantitative data to develop macroscopic models of diffusion since MD simulations allow to obtain diffusion coefficients for different species confined in pores with variable size, ranging from interlayer spaces (below 1 nm) to macropores of hundreds of nm.

Acknowledgments

This work was supported by the Department of Education, Language Policy and Culture of the Basque Government (IT912-16) and the ELKARTEK program. The first author acknowledges the DOKBERRI 2019 I fellowship from the UPV/EHU. Part of this work was financially supported by the Japan Society for the Promotion of Science (JSPS, No. 17H03292). The authors also thank the technical and human support provided by IZO-SGI SGIker of UPV/EHU and European funding (ERDF and ESF), as well as the i2basque computing resources.

References

- Abriel, W., (1983). "Calcium sulfat subhydrat, $\text{CaSO}_4 \cdot 0,8\text{H}_2\text{O}$." *Acta Crystallographica*, C39(8), 956-958. (in German)
- Al-Amoudi, O. S. B., (2002). "Attack on plain and blended cements exposed to aggressive sulfate environments." *Cement and Concrete Composites*, 24(3-4), 305-316.
- Amano, H., Akiyama, M., Chunlei, B., Kawamura, T., Kishimoto, T., Kuroda, T., Muroi, T., Odaira, T., Ohta, Y. and Takeda, K., (2012). "Radiation measurements in the Chiba Metropolitan Area and radiological aspects of fallout from the Fukushima Dai-ichi Nuclear Power Plants accident." *Journal of Environmental Radioactivity*, 111, 42-52.
- Androniuk, I., Landesman, C., Henocq, P. and Kalinichev, A. G., (2017). "Adsorption of gluconate and uranyl on CSH phases: Combination of wet chemistry experiments and molecular dynamics simulations for the binary systems." *Physics and Chemistry of the Earth*, 99, 194-203.
- Atkinson, A. and Hearne, J. A., (1989). "Mechanistic model for the durability of concrete barriers exposed to sulphate-bearing groundwaters." *MRS Online Proceedings Library Archive*, 176, Article No. 149.
- Atkinson, A. and Nickerson, A. K., (1984). "The diffusion of ions through water-saturated cement." *Journal of Materials Science*, 19(9), 3068-3078.
- Bagosi, S. and Csetényi, L. J., (1998). "Caesium immobilisation in hydrated calcium-silicate-aluminate systems." *Cement and Concrete Research*, 28(12), 1753-1759.
- Bako, I., Hutter, J. and Palinkas, G., (2002). "Car-Parrinello molecular dynamics simulation of the hydrated calcium ion." *Journal of Chemical Physics*, 117(21), 9838-9843.
- Barinov, A. S., Ozhovan, M. I., Sobolev, I. A. and Ozhovan, N. V., (1990). "Potential hazard of solidified radioactive wastes." *Radiokhimiya*, 32(4), 127-131.
- Bonaccorsi, E., Merlino, S. and Kampf, A. R., (2005). "The crystal structure of tobermorite 14 \AA (Plombierite), a C-S-H phase." *Journal of the American Ceramic Society*, 88(3), 505-512.
- Bonnaud, P. A., Manzano, H., Miura, R., Suzuki, A., Miyamoto, N., Hatakeyama, N. and Miyamoto, A., (2016). "Temperature dependence of nanoconfined water properties: Application to cementitious materials." *The Journal of Physical Chemistry C*, 120(21), 1465-11480.
- Brehm, M. and Kirchner, B., (2011). "TRAVIS - A free analyzer and visualizer for Monte Carlo and molecular dynamics trajectories." *Journal of Chemical Information and Modeling*, 51(8), 2007-2023.
- Brooks, B. R., Bruccoleri, R. E., Olafson, B. D., States, D. J., Swaminathan, S. and Karplus, M., (1983). "CHARMM: a program for macromolecular energy, minimization, and dynamics calculations." *Journal of Computational Chemistry*, 4(2), 187-217.
- Chen, J. J., Thomas, J. J., Taylor, H. F. W. and Jennings, H. M., (2004). "Solubility and structure of calcium silicate hydrate." *Cement and Concrete Research*, 34(9), 1499-1519.
- Chenoweth, K., Van Duin, A. C. T. and Goddard, W. A., (2008). "ReaxFF reactive force field for molecular dynamics simulations of hydrocarbon oxidation." *The Journal of Physical Chemistry A*, 112(5), 1040-1053.
- Chiu, Y.-C., Liu, W.-R., Chang, C.-K., Liao, C.-C., Yeh, Y.-T., Jang, S.-M. and Chen, T.-M., (2010). " $\text{Ca}_2\text{PO}_4\text{Cl}:\text{Eu}^{2+}$: An intense near-ultraviolet converting blue phosphor for white light-emitting diodes." *Journal of Materials Chemistry*, 20(9), 1755-1758.
- Cong, X. and Kirkpatrick, R. J., (1996). " ^{29}Si MAS NMR study of the structure of calcium silicate

- hydrate." *Advanced Cement Based Materials*, 3(3-4), 144-156.
- Coumes, C. C. D. and Courtois, S., (2003). "Cementation of a low-level radioactive waste of complex chemistry: Investigation of the combined action of borate, chloride, sulfate and phosphate on cement hydration using response surface methodology." *Cement and Concrete Research*, 33(3), 305-316.
- Cuesta, A., Zea-Garcia, J. D., Londono-Zuluaga, D., Angeles, G., Santacruz, I., Vallcorba, O., Dapiaggi, M., Sanf elix, S. G. and Aranda, M. A. G., (2018). "Multiscale understanding of tricalcium silicate hydration reactions." *Nature Scientific Reports*, 8(1), 1-11.
- Cygan, R. T., Liang, J.-J. and Kalinichev, A. G., (2004). "Molecular models of hydroxide, oxyhydroxide, and clay phases and the development of a general force field." *The Journal of Physical Chemistry B*, 108(4), 1255-1266.
- Dolado, J. S., Griebel, M. and Hamaekers, J., (2007). "A molecular dynamic study of cementitious calcium silicate hydrate (C-S-H) gels." *Journal of the American Ceramic Society*, 90(12), 3938-3942.
- Duque-Redondo, E., Yamada, K., L opez-Arbeloa, I. and Manzano, H., (2018a). "Adsorption and diffusion of Na⁺, Cs⁺ and Ca²⁺ ions in CSH and CaSH nanopores." *Chemrxiv*, Article No. 6476510.
- Duque-Redondo, E., Yamada, K., L opez-Arbeloa, I. and Manzano, H., (2018b). "Cs-137 immobilization in C-S-H gel nanopores." *Physical Chemistry Chemical Physics*, 20(14), 9289-9297.
- Duque-Redondo, E., Yamada, K. and Manzano, H., (2021). "Cs retention and diffusion in C-S-H at different Ca/Si ratio." *Cement and Concrete Research*, 140, Article ID 106294.
- Einstein, A., (1905). "About the motion of particles suspended in liquids at rest, required by the molecular kinetic theory of heat." *Annalen der Physik*, 322(8), 549-560. (in German)
- El-Kamash, A. M., El-Dakroury, A. M. and Aly, H. F., (2002). "Leaching kinetics of ¹³⁷Cs and ⁶⁰Co radionuclides fixed in cement and cement-based materials." *Cement and Concrete Research*, 32(11), 1797-1803.
- Ewald, P. P., (1921). "The calculation of optical and electrostatic grid potentials." *Annalen der Physik*, 369(3), 253-287. (in German)
- Fogarty, J. C., Aktulga, H. M., Grama, A. Y., van Duin, A. C. T. and Pandit, S. A., (2010). "A reactive molecular dynamics simulation of the silica-water interface." *Journal of Chemical Physics*, 132(17), Article No. 174704.
- Fujii, K. and Kondo, W., (1981). "Heterogeneous equilibrium of calcium silicate hydrate in water at 30°C." *Journal of the Chemical Society Dalton Transactions*, 2, 645-651.
- Glasser, F. P., (1993). "Chemistry of cement-solidified waste forms." In: R. D. Spence, Ed. *Chemistry and Microstructure of Solidified Waste Forms*. Boca Raton, Florida USA: Lewis Publishers, 1-39.
- Glasser, F. P. and Atkins, M., (1994). "Cements in radioactive waste disposal." *MRS Bulletin*, 19(12), 33-38.
- Guggenheim, E. A., (1985). "*Thermodynamics - An advanced treatment for chemists and physicists*." Amsterdam: North-Holland Physics Publishing.
- Hewlett, P., (2003). "*Lea's chemistry of cement and concrete*." 4th ed. Oxford: Butterworth-Heinemann.
- Hofer, T. S., Tran, H. T., Schwenk, C. F. and Rode, B. M., (2004). "Characterization of dynamics and reactivities of solvated ions by ab initio simulations." *Journal of Computational Chemistry*, 25(2), 211-217.
- Jantunen, M., Reponen, A., Kauranen, P. and Vartiainen, M., (1991). "Chernobyl fallout in southern and central Finland." *Health Physics*, 60(3), 427-434.
- Jiang, J., Wang, P. and Hou, D., (2017). "The mechanism of cesium ions immobilization in the nanometer channel of calcium silicate hydrate: A molecular dynamics study." *Physical Chemistry Chemical Physics*, 19(41), 27974-27986.
- Johnston, H. M. and Wilmot, D. J., (1992). "Sorption and diffusion studies in cementitious grouts." *Waste Management*, 12(2-3), 289-297.
- Kalinichev, A. G., Wang, J. W. and Kirkpatrick, R. J., (2007). "Molecular dynamics modeling of the structure, dynamics and energetics of mineral-water interfaces: Application to cement materials." *Cement and Concrete Research*, 37, 337-347.
- Kiran, R., Samouh, H., Igarashi, G., Haji, T., Ohkubo, T., Tomita, S. and Maruyama, I., (2020). "Temperature-dependent water redistribution from large pores to fine pores after water uptake in hardened cement paste." *Journal of Advanced Concrete Technology*, 18(10), 588-599.
- Kluger, W., Hild, W., K oster, R., Meier, G. and Krause, H., (1980). "*Bituminization of radioactive waste concentrates from reprocessing, nuclear research establishments and nuclear power plants*." Karlsruhe, Germany: Kernforschungszentrum Karlsruhe GmbH. (in German)
- Kova evi , G., Nicoleau, L., Nonat, A. and Veryazov, V., (2016). "Revised atomistic models of the crystal structure of C-S-H with high C/S ratio." *Zeitschrift f ur Physikalische Chemie*, 230(9), 1411-1424.
- Kova evi , G., Persson, B., Nicoleau, L., Nonat, A. and Veryazov, V., (2015). "Atomistic modeling of crystal structure of Ca_{1.67}SiH_x." *Cement and Concrete Research*, 67, 197-203.
- Krishnamoorthy, T. M., Joshi, S. N., Doshi, G. R. and Nair, R. N., (1993). "Desorption kinetics of radionuclides fixed in cement matrix." *Nuclear Technology*, 104(3), 351-357.
- Krynicky, K., Green, C. D. and Sawyer, D. W., (1978). "Pressure and temperature dependence of self-diffusion in water." *Faraday Discussions of the Chemical Society*, 66, 199-208.

- Kubillus, M., Kubař, T., Gaus, M., Rezac, J. and Elstner, M., (2014). "Parameterization of the DFTB3 method for Br, Ca, Cl, F, I, K, and Na in organic and biological systems." *Journal of Chemical Theory and Computations*, 11(1), 332-342.
- Kumar, A., Walder, B. J., Kunhi Mohamed, A., Hofstetter, A., Srinivasan, B., Rossini, A. J., Scrivener, K., Emsley, L. and Bowen, P., (2017). "The atomic-level structure of cementitious calcium silicate hydrate." *The Journal of Physical Chemistry C*, 121(32), 17188-17196.
- Lee, W. E., Ojovan, M. I., Stennett, M. C. and Hyatt, N. C., (2006). "Immobilisation of radioactive waste in glasses, glass composite materials and ceramics." *Advances in Applied Ceramics*, 105(1), 3-12.
- Macásek, F., (1999). "Sorption and leaching properties of the composites and complexes of natural microporous materials." In: P. Misaelides, F. Macásek, T. J. Pinnavaia and C. Colella, Eds. *Natural Microporous Materials in Environmental Technology*. Dordrecht, The Netherlands: Springer, 109-135.
- Mähler, J. and Persson, I., (2011). "A study of the hydration of the alkali metal ions in aqueous solution." *Inorganic Chemistry*, 51(1), 425-438.
- Mahoney, M. W. and Jorgensen, W. L., (2001). "Diffusion constant of the TIP5P model of liquid water." *The Journal of Chemical Physics*, 114(1), 363-366.
- Manzano, H., Moeini, S., Marinelli, F., van Duin, A. C. T., Ulm, F.-J. and Pellenq, R. J. M., (2012a). "Confined water dissociation in microporous defective silicates: mechanism, dipole distribution, and impact on substrate properties." *Journal of the American Chemical Society*, 134(4), 2208-2215.
- Manzano, H., Pellenq, R. J. M., Ulm, F.-J., Buehler, M. J. and van Duin, A. C. T., (2012b). "Hydration of calcium oxide surface predicted by reactive force field molecular dynamics." *Langmuir*, 28(9), 4187-4197.
- Martínez, J. M. and Martínez, L., (2003). "Packing optimization for automated generation of complex system's initial configurations for molecular dynamics and docking." *Journal of Computational Chemistry*, 24(7), 819-25.
- Martínez, L., Andrade, R., Birgin, E. G. and Martínez, J. M., (2009). "*PACKMOL: A package for building initial configurations for molecular dynamics simulations*." Hoboken, New Jersey, USA: Wiley Subscription Services, Inc.
- Miyake, M., Komarneni, S. and Roy, R., (1989). "Kinetics, equilibria and thermodynamics of ion exchange in substituted tobermorites." *Materials Research Bulletin*, 24(3), 311-320.
- Neville, A., (1995). "Chloride attack of reinforced concrete: An overview." *Materials and Structures*, (2), Article No. 63.
- Ochs, M., Mallants, D. and Wang, L., (2015). "*Radionuclide and metal sorption on cement and concrete*." Cham, Switzerland: Springer International Publishing.
- Palmer, J. D. and Fairhall, G. A., (1992). "Properties of cement systems containing intermediate level wastes." *Cement and Concrete Research*, 22(2-3), 325-330.
- Payne, T. E., Brendler, V., Ochs, M., Baeyens, B., Brown, P. L., Davis, J. A., Ekberg, C., Kulik, D. A., Lutzenkirchen, J. and Missana, T., (2013). "Guidelines for thermodynamic sorption modelling in the context of radioactive waste disposal." *Environmental Modelling & Software*, 42, 143-156.
- Pinson, M. B., Masoero, E., Bonnaud, P. A., Manzano, H., Ji, Q., Yip, S., Thomas, J. J., Bazant, M. Z., Van Vliet, K. J. and Jennings, H. M., (2015). "Hysteresis from multiscale porosity: modeling water sorption and shrinkage in cement paste." *Physical Review Applied*, 3(6), Article No. 64009.
- Plimpton, S., (1995). "Fast parallel algorithms for short-range molecular dynamics." *Journal of Computational Physics*, 117(1), 1-19.
- Qomi, M. J. A., Bauchy, M., Ulm, F.-J. and Pellenq, R. J.-M., (2014). "Anomalous composition-dependent dynamics of nanoconfined water in the interlayer of disordered calcium-silicates." *The Journal of Chemical Physics*, 140(5), Article No. 054515.
- Qomi, M. J. A., Krakowiak, K. J., Bauchy, M., Stewart, K. L., Shahsavari, R., Jagannathan, D., Brommer, D. B., Baronnet, A., Buehler, M. J., Yip, S., Ulm, F.-J., Van Vliet, K. J. and Pellenq, R. J. M., (2014). "Combinatorial molecular optimization of cement hydrates." *Nature Communications*, 5, Article No. 5960.
- Rahman, R. O. A., Rakhimov, R. Z., Rakhimova, N. R. and Ojovan, M. I., (2014). "*Cementitious materials for nuclear waste immobilization*." Sussex, UK: John Wiley & Sons Ltd.
- Ramezaniyanpour, A. A. and Riahi Dehkordi, E., (2017). "Effect of combined sulfate-chloride attack on concrete durability - A review." *AUT Journal of Civil Engineering*, 1(2), 103-110.
- Real, A., Sundell-Bergman, S., Knowles, J. F., Woodhead, D. S. and Zinger, I., (2004). "Effects of ionising radiation exposure on plants, fish and mammals: relevant data for environmental radiation protection." *Journal of Radiological Protection*, 24(4A), 123-137.
- Real, J., Persin, F. and Camarasa-Claret, C., (2002). "Mechanisms of desorption of ¹³⁴Cs and ⁸⁵Sr aerosols deposited on urban surfaces." *Journal of Environmental Radioactivity*, 62(1), 1-15.
- Rejmak, P., Dolado, J. S., Stott, M. J. and Ayuela, A., (2012). "²⁹Si NMR in cement: A theoretical study on calcium silicate hydrates." *The Journal of Physical Chemistry*, 116(17), 9755-9761.
- Schwenk, C. F., Hofer, T. S. and Rode, B. M., (2004). "'Structure breaking' effect of hydrated Cs⁺." *The Journal of Physical Chemistry A*, 108(9), 1509-1514.
- Shahsavari, R., Pellenq, R. J.-M. and Ulm, F.-J., (2011). "Empirical force fields for complex hydrated

- calcio-silicate layered materials.” *Physical Chemistry Chemical Physics*, 13(3), 1002-1011.
- Stroh, J., Meng, B. and Emmerling, F., (2016). “Deterioration of hardened cement paste under combined sulphate-chloride attack investigated by synchrotron XRD.” *Solid State Sciences*, 56, 29-44.
- Thomas, J. J., Chen, J. J., Jennings, H. M. and Neumann, D. A., (2003). “Ca-OH bonding in the C-S-H gel phase of tricalcium silicate and white portland cement pastes measured by inelastic neutron scattering.” *Chemistry of Materials*, 15(20), 3813-3817.
- Vanommeslaeghe, K., Hatcher, E., Acharya, C., Kundu, S., Zhong, S., Shim, J., Darian, E., Guvench, O., Lopes, P. and Vorobyov, I., (2010). “CHARMM general force field: A force field for drug-like molecules compatible with the CHARMM all-atom additive biological force fields.” *Journal of Computational Chemistry*, 31(4), 671-690.
- Verlet, L., (1967). “Computer ‘experiments’ on classical fluids, I: Thermodynamical properties of Lennard-Jones molecules.” *Physical Review*, 159(1), 98-103.
- Volchek, K., Miah, M. Y., Kuang, W., DeMaleki, Z. and Tezel, F. H., (2011). “Adsorption of cesium on cement mortar from aqueous solutions.” *Journal of Hazardous Materials*, 194, 331-337.
- Yuan-Hui, L. and Gregory, S., (1974). “Diffusion of ions in sea water and in deep-sea sediments.” *Geochimica et Cosmochimica Acta*, 38(5), 703-714.
- Zachariasen, W. H., (1948). “Crystal chemical studies of the 5f-series of elements, II: The crystal structure of Cs_2PuCl_6 .” *Acta Crystallographica*, 1(5), 268-269.